Available online at www.sciencedirect.com
ScienceDirect
Polymer 49 (2008) 570–578
polymer
www.elsevier.com/locate/polymer

Influence of polymer modulus on the percolation threshold of latex-based composites

Yeon Seok Kim, John B. Wright, Jaime C. Grunlan*

Department of Mechanical Engineering, Texas A&M University, College Station, TX 77843-3123, United States

Received 27 August 2007; received in revised form 16 November 2007; accepted 18 November 2007
Available online 22 November 2007

Abstract

Monodispersed copolymer emulsions with different glass transition temperatures were synthesized to investigate the effect of room temperature polymer matrix modulus on the electrical properties of carbon black (CB) filled segregated network composites. The emulsion with the highest modulus at room temperature produced composites with the lowest percolation threshold. The threshold for a composite made from a copolymer latex containing an equal ratio of butyl acrylate and methyl methacrylate (BA5) is 1.5 vol%, while the percolation threshold for the much lower modulus BA7 (7:3 BA/MMA ratio) is 4.93 vol%. The microstructure of each composite shows significant differences in the level of CB dispersion within the polymer matrix. Higher modulus polymer particles push the CB more efficiently into the interstitial space between them, resulting in a lower percolation threshold. This modulus effect was confirmed by increasing the drying temperature, where the moduli of latexes (BA5, BA5.5, and BA6) were more similar and the percolation thresholds for three composites also become closer to one another.

Keywords: Segregated network; Percolation threshold; Matrix modulus

1. Introduction

Polymer composites containing electrically conductive filler combine the beneficial properties inherited from the polymer matrix (good toughness, flexibility, light weight) with electrical conductivity. These materials are useful for applications such as thermal resistors [1,2], chemical sensors [3,4], electromagnetic interference (EMI) shielding [5,6], and electrostatic dissipation (ESD) [6,7]. Despite their promise, a high concentration of conductive filler is often required for these composites to achieve reasonable conductivity. Greater processing viscosity and more brittle final composites accompany large filler concentration [8]. Segregated network composites, made with a polymer blend or a particulate polymer matrix, solve this problem by reducing the percolation threshold [9–22]. The percolation threshold is the amount of filler at which the conductivity of a composite significantly increases due to the formation of an interconnected network [23]. It has been reported that the percolation threshold for randomly dispersed carbon black is around 15 vol% [24,25], but composites with a segregated network have achieved percolation thresholds below 0.1 vol% [22].

The segregated network concept was initially formalized by Kusy in the context of lightly hot pressing dry mixtures of polymer and metal powders to create electrically conductive composites [26]. In essence, the conductive filler is given a restricted volume in which to reside that leads to network formation at low concentration. Using an immiscible polymer blend is one of the most common techniques used to form a segregated network and relies on the conductive filler being dispersed predominantly within one polymer [9–12] or at the interface between the two polymers [9,13–15]. A simpler method uses a polymer emulsion to create the segregated network by forcing the conductive particles into the interstitial space between the solid polymer particles during drying [16–21], as illustrated in Fig. 1. The emulsion particles are relatively large (typically

* Corresponding author. Tel.: +1 979 845 3027; fax: +1 979 862 3989.
E-mail address: jgrunlan@tamu.edu (J.C. Grunlan).

0032-3861/$ - see front matter © 2007 Elsevier Ltd. All rights reserved.
doi:10.1016/j.polymer.2007.11.035

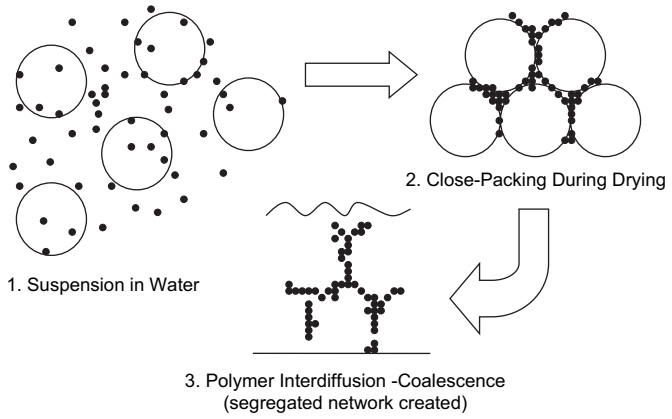

Fig. 1. Schematic illustration of producing a polymer nanocomposite with a segregated network from an aqueous mixture of carbon black and a polymer emulsion.

100 nm–10 μm) compared to the size of conductive filler, which significantly lowers the percolation threshold of the final composite. This method is similar to using immiscible polymer blends in terms of creating excluded volume where little or no conductive particles reside. Unlike with a polymer blend, which is melt processed and has multiple phases, an emulsion has only a single polymer phase and processing can be done at room temperature [16,18].

Electrically conductive polymer composites are typically produced by melt [27,28] or solution-based processing [29,30], which makes the polymer modulus negligible during processing. When using a polymer emulsion, the matrix remains solid throughout the processing steps. This is why the polymer modulus will play a key role in the final composite microstructure and ultimately influence electrical conductivity. In this work, the influence of emulsion polymer modulus on the electrical properties of carbon black-filled composites is examined. Monodisperse acrylic latexes with varying glass transition temperature were synthesized and used as the composite matrix starting material. Polymers with varying glass transition temperatures were made by changing the ratio of methyl methacrylate to butyl acrylate in the emulsion, which produced variations in room temperature polymer modulus (i.e., greater T_g polymer has greater modulus). Composites prepared with lower room temperature modulus emulsion exhibit a greater percolation threshold due to greater deformability of the polymer particles. These results reveal an additional parameter for tailoring the percolation threshold that may be useful for a variety of applications requiring flexible conductive films.

2. Experimental

2.1. Materials

Methyl methacrylate (MMA), *n*-butyl acrylate (BA), methacrylic acid (MAA), poly(vinyl alcohol) (PVOH, M_n 85,000–124,000 g/mol), and sodium persulfate ($Na_2S_2O_8$) were purchased from Sigma–Aldrich (Milwaukee, WI) and used as received. Triton X-405 (70% in water solution), from Sigma–Aldrich, and sodium dodecyl sulfate (SDS, $C_{12}H_{25}NaO_4S$), from J.T. Baker (Phillipsburg, NJ), were used as surfactants. Triton X-405 is an octylphenol ethoxylate surfactant that provides steric stabilization, which improves the colloidal and thermal stabilities of polymer emulsions [31]. Sodium bicarbonate ($NaHCO_3$), from Sigma–Aldrich, was used as a buffer during polymerization and later used to adjust the pH of the final latexes. Conductex 7055 Ultra carbon black (CB) was provided by Columbian Chemicals (Marietta, GA). This CB has a nitrogen surface area (NSA) of 55 m^2/g and a primary particle size of 42 nm. Sodium silicate ($Na_2O_7Si_3$), from Sigma–Aldrich, and Tamol 791 A, from Rohm and Haas (Philadelphia, PA) were used as dispersing agents for carbon black.

2.2. Emulsion polymer synthesis

Emulsions (or latexes) were synthesized using a semi-continuous polymerization process. Synthesis was carried out in a 1000 mL three-neck round bottom flask equipped with a mechanical stirrer, a Teflon stirring paddle, and a speed controller. To begin, 9.23 g of Triton X-405 was dissolved in 37.59 g of deionized water. Once dissolved, a mixture of BA, MMA, and MAA was continuously fed into the flask for 45 min at room temperature while the mixture was stirred at 350 rpm. This pre-emulsion, a highly viscous white blend, was then moved into the addition funnel for polymerization. Triton X- 405, SDS, and sodium bicarbonate were dissolved in water in the reaction flask, fitted with a condenser, addition funnel and a nitrogen gas tube. The solution was stirred at 155 rpm and a mixture of BA and MMA (44.63 g) was added into the flask. Next, the flask was heated to 65 °C using a water bath to keep the temperature constant during the reaction. Once at 65 °C, the polymerization was initiated by adding a sodium persulfate solution. After 5 min, the pre-emulsion was steadily dripped into the flask for 3.5 h. The reactor was held at 65 °C for 15 min after the pre-emulsion feed was complete to reduce the amount of unreacted monomer. At the end of the polymerization, the latexes were filtered through 10 μm polyester filter bags to remove grit. Poly(vinyl alcohol) (PVOH) was then added to the latexes (2% by weight of acrylic polymer) to improve their shear stability during the mixing process [32] and sodium bicarbonate was used to increase the pH of latexes to 7.5. Films for glass transition temperature and modulus measurement were prepared by drying the latexes under ambient condition for two days, followed by drying in a vacuum desiccator for an additional 24 h. Compositions of the pre-emulsions and reactor charges for all of the latexes synthesized are shown in Table 1.

2.3. Composite preparation

Sodium silicate (0.05 wt%) and Tamol 731A (0.05 wt%) were added to deionized water and carbon black was then added at a concentration of 5 wt% using a high speed impeller for 20 min at 3600 rpm, followed by rolling in a bottle at 10 rpm for 12 h to achieve equilibrium. This CB suspension was then added to each emulsion, along with deionized water,

Table 1
Recipe for the latexes with various ratios of BA/MMA

Pre-emulsion					
Latex	BA (g)	MMA (g)	MAA (g)	Triton X-405 (g)	Deionized water (g)
BA5	101.64	101.64	5.05	9.23	37.59
BA5.5	111.91	91.48	5.05	9.23	37.59
BA6	121.97	81.31	5.05	9.23	37.59
BA7	142.30	60.99	5.05	9.23	37.59

Reactor charge							
Latex	BA (g)	MMA (g)	Triton X-405 (g)	SDS (g)	Sodium persulfate (g)	Sodium bicarbonate (g)	Deionized water (g)
BA5	22.31	22.31	5.10	0.36	1.02	1.02	202.73
BA5.5	24.54	20.08	5.10	0.36	1.02	1.02	202.73
BA6	26.78	17.85	5.10	0.36	1.02	1.02	202.73
BA7	31.24	13.39	5.10	0.36	1.02	1.02	202.73

and mixed at 3600 rpm for 15 min. The mixture having the highest concentration of CB was made first, with lower concentration made by diluting with deionized water and more polymer emulsion. These aqueous pre-composite mixtures were kept at a constant 15 wt% solids during processing. After the mixing was complete, 12 g of this mixture was poured into a 58 cm^2 mold and allowed to dry under ambient conditions for two days, followed by another 24 h in a vacuum desiccator. The final composite films have a thickness of 185–230 μm.

2.4. Emulsion and composite characterization

Polymer particle size analysis was performed with a Zetasizer Nano-S Zen 1600 (Malvern Inc., Southborough, MA). A Q-800 Dynamic Mechanical Analyzer (DMA) (TA Instruments, New Castle, DE) was used to evaluate the glass transition temperature and storage modulus of the dry latex-based films. DMA testing was conducted with a tensile fixture at a fixed frequency of 1 Hz. The temperature was ramped from −50 to 90 °C with a heating rate of 3 °C/min. The amplitude of the strain was fixed at 0.1%. The maximum point on the loss modulus was taken to be the glass transition temperature (T_g) for each sample (ASTM 1640-04). Cross-sections of the composite films were imaged with a Tescan VEGA-II SEM (Cranberry Township, PA). Films were soaked in liquid nitrogen and fractured by hand and the surfaces were sputter coated with 4 nm of platinum prior to SEM imaging. Electrical conductivity was measured with a home-built four-point-probe system.

3. Results and discussion

3.1. Monodispersed latex characterizations

Following emulsion polymerization, the particle size and glass transition temperature of the polymers were characterized. All samples were dried at room temperature. Particle size, BA/MMA ratio, glass transition temperature and storage moduli of these latexes are summarized in Table 2. All of the latexes have an average particle size of approximately 150 nm, with a distribution narrow enough to be called monodisperse (<1.1) [33]. The combination of an ionic and nonionic surfactant typically yields emulsions with a narrow particle size distribution [34]. Fig. 2 shows the experimental and theoretical glass transition temperatures for these latexes. The glass transition temperatures were initially estimated using the Fox equation [35]:

$$\frac{1}{T_g} = \frac{w_1}{T_{g1}} + \frac{w_2}{T_{g2}} + \frac{w_3}{T_{g3}} = \frac{w_{BA}}{219} + \frac{w_{MMA}}{378} + \frac{w_{MAA}}{282} \quad (1)$$

where, w is the weight fraction of each polymer and T_g is the glass transition temperature of each homopolymer and copolymer in Kelvin. The experimental data are in qualitative agreement with the Fox prediction in that the slope of Eq. (1) matches the experimentally observed increase of the glass transition temperature, although experimentally determined T_gs are consistently 12–15 °C higher than the Fox prediction. This discrepancy is likely due to the different sequencing arrangements of MMA and BA repeat units. The Fox equation assumes that the two monomers are arranged in a completely random manner, but MMA has a higher reactivity ratio ($r_{MMA} = 0.920$ and $r_{BA} = 0.130$) [36], so it tends to react with itself more than BA during polymerization. This difference in reactivity will lead to longer sequences of MMA, making the glass transition temperature of the copolymer higher than expected.

Fig. 3 shows latex storage moduli as a function of temperature. Polymer storage modulus is comparable to elastic modulus at room temperature [37]. Room temperature storage modulus increases with glass transition temperature as expected. The storage modulus at 20 °C is 640 MPa for BA5, 70 MPa for BA5.5, 18 MPa for BA6, and 3.6 MPa for BA7, respectively. By changing the BA/MMA ratio from 1:1 (BA5) to 5.5:4.5 (BA5.5), the storage modulus at room temperature drops nearly one order of magnitude due to the transition between the glassy and rubbery states of the polymer. It is worth noting that the

Table 2
Composition, particle size, T_g, and moduli of the latexes

Latex	BA/MMA	Particle size (nm)	PDI	T_g (°C)	E'^a (MPa)	E'^b (MPa)
BA5	50:50	150	1.057	20.2	640	0.84
BA5.5	55:45	147	1.026	10.7	70	0.63
BA6	60:40	149	1.037	0.4	18	0.51
BA7	70:30	149	1.061	−8.7	3.6	0.1

[a] Storage modulus measured at 20 °C.
[b] Storage modulus measured at 80 °C.

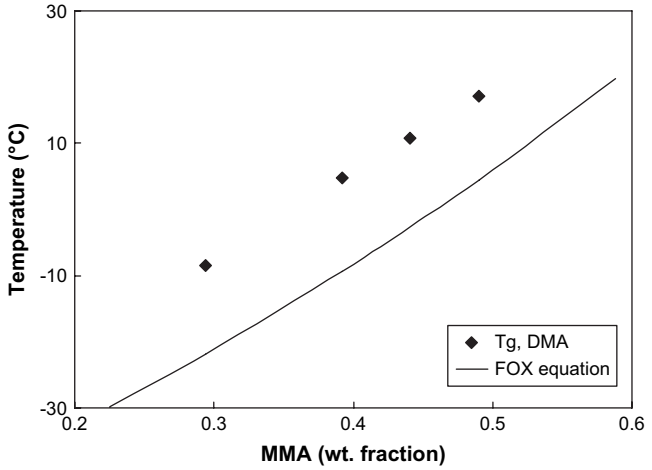

Fig. 2. Glass transition temperature of P(MMA-*co*-BA) copolymers, measured experimentally and predicted by the Fox equation, as a function of the weight fraction of methyl methacrylate.

overall shape of the storage modulus curve is similar for all of the latexes despite differences in chemical composition. This suggests that the thermo-mechanical response of all latexes is very similar, regardless of the glass transition temperature. Additionally, the storage modulus curve drops only once for each polymer, suggesting that BA and MMA are completely miscible with each other, making one coherent phase.

3.2. Composite microstructure

After polymerization, carbon black was added to each emulsion to produce electrically conductive composites. During drying, the polymer particles push the CB into the interstitial space between them and the segregated CB network is formed [16,17]. The modulus of the polymer particle plays an important role in the formation of this segregated network. Fig. 4 shows freeze fractured cross-sections of composites dried at room temperature. At this temperature, BA5 has the highest modulus (Table 2), which is two orders of magnitude higher than that of the lowest (BA7). The BA5 composites have heavily aggregated strands of carbon black at

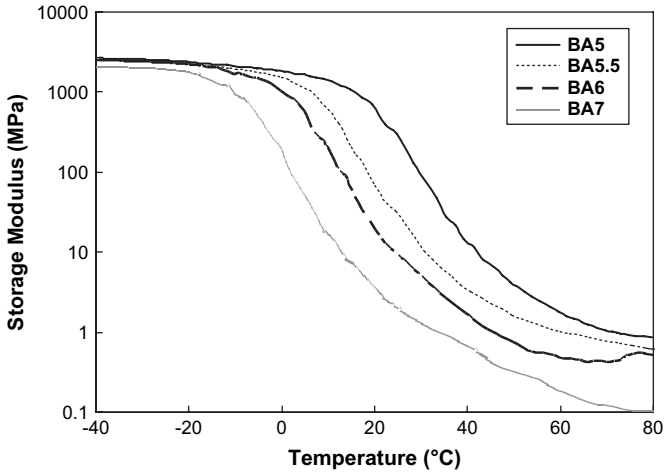

Fig. 3. Storage modulus (E') of acrylic latexes as a function of temperature.

a concentration of 5 wt%, which are part of a strong three dimensional network (Fig. 4(a)). As the amount of butyl acrylate in the matrix increases, the matrix modulus decreases and carbon black is more randomly distributed. Before drying, the dispersion level of CB in each emulsion is comparable because CB is predispersed in water using the same dispersing agents and mixing speed. The difference in CB distribution within each polymer matrix comes from the differing moduli during drying. The copolymer containing a 1:1 BA/MMA ratio (BA5) has a relatively high modulus at room temperature, so the polymer particles tend to maintain their original shape and more effectively force CB into the interstitial space during coalescence. As a result, a segregated network of CB is formed at much lower concentration relative to the other systems. BA6 and BA7 (6:4 and 7:3 BA/MMA ratio, respectively) have very low moduli compared to the other latexes, so the polymer is much softer and the emulsion particles tend to deform around CB rather than simply touching them. The polymer matrix is better able to penetrate into the gaps between CB particles and disrupt the formation of a conducting pathway. SEM images of BA6 and BA7 with 5 wt% CB (Fig. 4(e) and (g)) show that CB particles are more separated by the polymer matrix. At this concentration, the electrical conductivity is not measurable for these systems, as discussed in the next section. BA5.5 composites show intermediate behavior between BA5 and BA6. The aggregation of CB is less severe than BA5, but carbon black still shows some level of aggregation and the SEM image (Fig. 4(c)) shows the early development of a segregated network structure. The images of composites with 10 wt% CB more clearly highlight the difference between these composites. For the BA5 system, CB is highly aggregated in the matrix due to the lack of polymer deformation around the filler particles. The segregated network of CB is well developed for BA5 and BA5.5 composites (Fig. 4(b) and (d)). The BA6 and BA7 composites containing 10 wt% CB (Fig. 4(f) and (h)) show a more random distribution of CB, but the segregated network is now clearly observed.

Composites were also dried at elevated temperature (80 °C) to further reduce the matrix modulus for all systems. Fig. 5 shows the cross-sectional images of these composites. At 80 °C, the storage modulus is 0.84 MPa for BA5, 0.63 MPa for BA5.5, 0.51 MPa for BA6, and 0.1 MPa for BA7. The dispersion level of CB in each matrix is much more similar due to the similar moduli. Due to the extremely low conductivity, the cross-sectional images of samples containing 5 wt% CB are not presented here. At 10 wt% CB, the SEM images of BA5, BA5.5, and BA6 show very similar microstructure (Fig. 5(a), (c) and (e)). The carbon black appears evenly distributed throughout the polymer matrix, although the segregated network is observable. With 15 wt% CB, all three composites show a well defined network structure of CB (Fig. 5(b), (d), and (f)). For the BA5.5 and BA6 composites, the dispersion level at 10 wt% CB (Fig. 5(c) and (e)) is comparable to that of the composites dried at room temperature (Fig. 4(d) and (f)) with the same concentration. In contrast, BA5 shows a dramatic difference in the distribution of CB between composites dried at these two temperatures. The composites dried at room

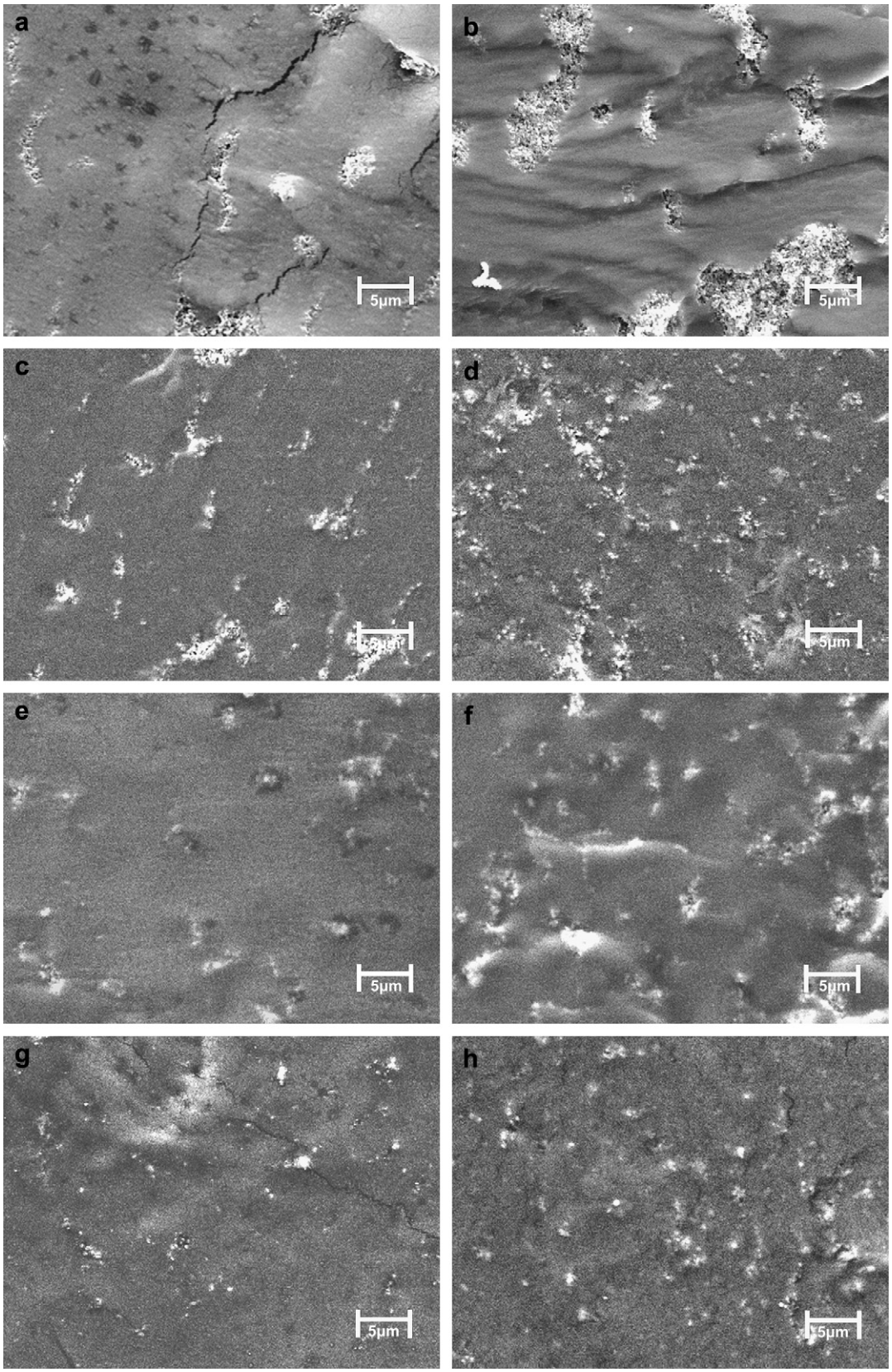

Fig. 4. SEM images of BA5 with 5 (a) and 10 wt% CB (b), BA5.5 with 5 (c) and 10 wt% CB (d), BA6 with 5 (e) and 10 wt% CB (f), and BA7 with 5 (g) and 10 wt% CB (h). These composites were dried at room temperature.

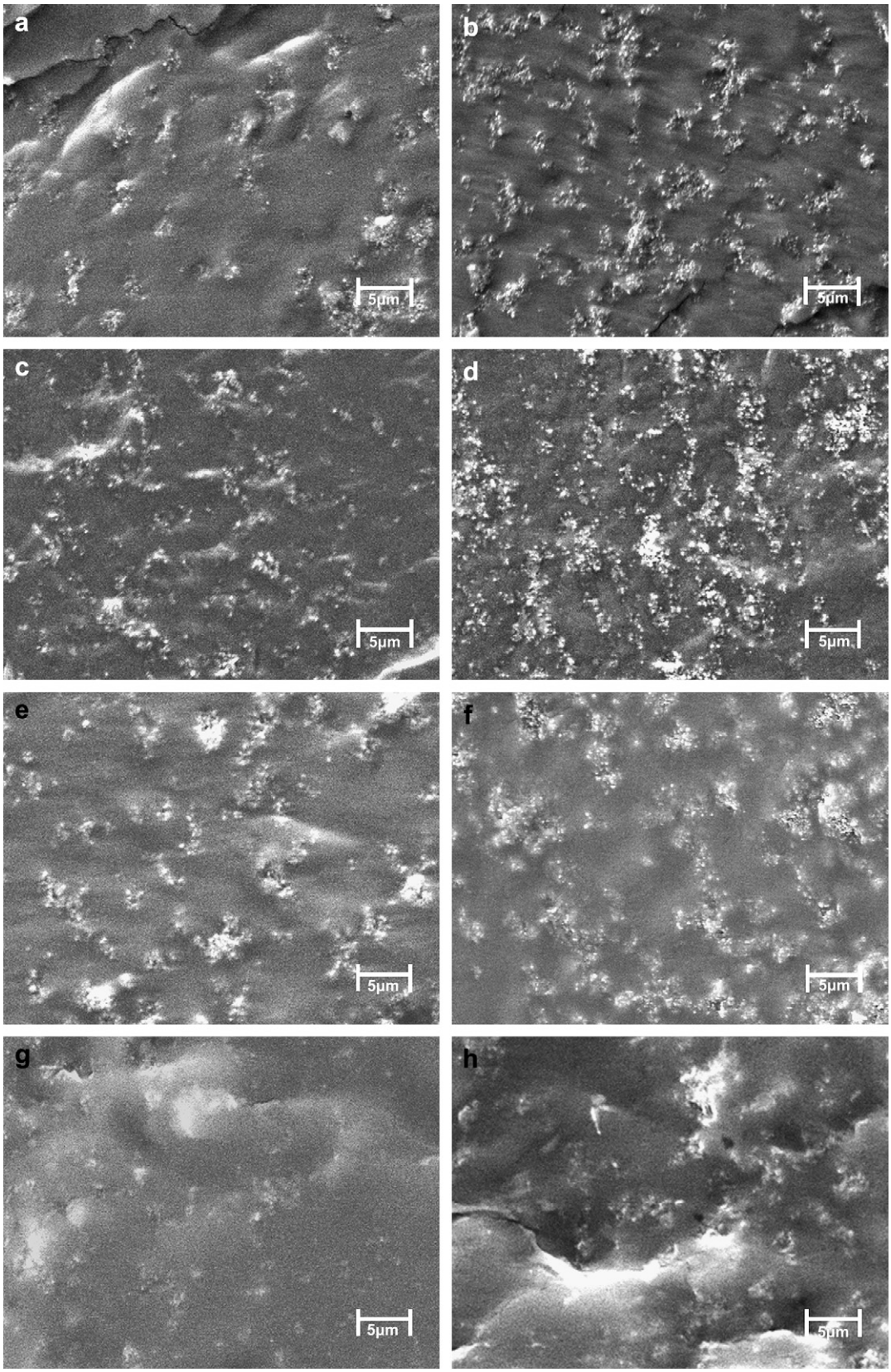

Fig. 5. SEM images of BA5 with 10 (a) and 15 wt% CB (b), BA5.5 with 5 (c) and 10 wt% CB (d), BA6 with 10 (e) and 15 wt% CB (f), and BA7 with 10 (g) and 15 wt% CB (h). These composites were dried at 80 °C.

temperature show a significant level of porosity due to CB aggregation. These pores are nearly eliminated when the drying temperature was raised to 80 °C due to the lower modulus of the emulsion particles that more effectively deform around the high modulus CB particles and fill the gaps between them. The BA7 composites show somewhat different behavior relative to the others. At room temperature, the dispersion level of CB is equivalent in BA6 and BA7. At 80 °C, the CB is almost randomly dispersed up to 15 wt% CB. At 10 wt% CB (Fig. 5(g)) no network structure has formed and only a weak network is observed at 15 wt% CB (Fig. 5(h)). The low glass transition temperature of BA7 (∼−9 °C) causes the emulsion particles to become very soft at 80 °C (E′ ∼ 0.1 MPa). These low modulus particles behave almost like a melt, easily separating CB particles and hindering the formation of a segregated network.

3.3. Composite electrical conductivity

Electrical conductivity was measured as a function of carbon black concentration for the four types of BA composites (see Table 2 for BA types) dried at room temperature and at 80 °C. These results are shown in Fig. 6(a) (room temperature) and Fig. 7(a) (80 °C). The carbon black concentration was converted to a volume fraction (expressed as vol%) using the known density of each homopolymer ($\rho_{PMMA} = 1.17$ g/cm^3 and $\rho_{PBA} = 1.087$ g/cm^3) and carbon black ($\rho_{CB} = 1.89$ g/cm^3). The percolation threshold (expressed as vol% CB) was obtained by fitting the percolation power law to the experimental conductivity–concentration data [23]:

$$\sigma = \sigma_0 (V - V_c)^s \quad (2)$$

where σ is the conductivity of the composite, σ_0 is the effective conductivity of the filler, V is the volume fraction of the filler, V_c is the percolation threshold, and s is the power-law exponent. At room temperature, BA5 has the lowest percolation threshold (1.5 vol%) and the conductivity values are higher for BA5 at all concentrations. The percolation threshold for all of the systems are below 5 vol%, which is a low value relative to the randomly dispersed, solution or melt-processed carbon black composites [24,25]. This is due to the formation of a segregated network of carbon black within the polymer matrix. As the modulus of the matrix increases, V_c decreases due to the more rigid polymer particles forcing the CB into the interstitial space more effectively, thereby forming the segregated network at a much lower concentration. The stronger CB network in BA5, due to the lack of polymer deformation and heavy aggregation of CB, results in this higher conductivity. The difference in the electrical conductivity between BA5 and other systems becomes smaller as the CB concentration increases. The percolation threshold for BA7 is close to that of BA6, but the conductivity values are much lower. It is interesting to note that a plot of T_g as a function of percolation threshold (Fig. 6(b)) intercepts 15 vol% CB (the value expected for random dispersion of a spherical filler [23]) at 204 K. This value of T_g would correspond to a melting temperature (T_m) of 306 K, assuming the $T_m/T_g = 1.5$ rule of thumb [35]. Therefore, this plot suggests

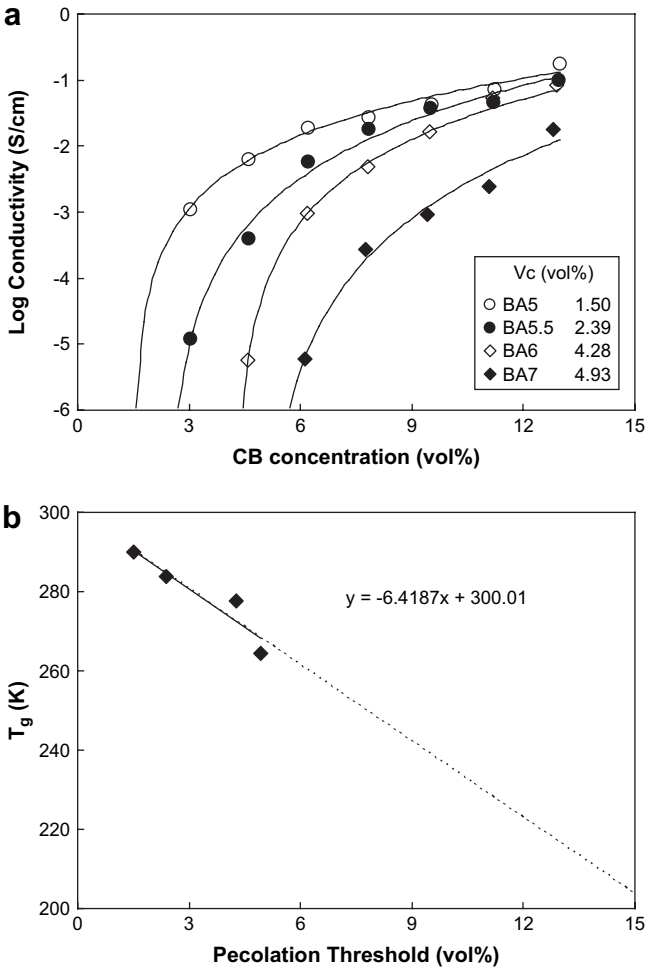

Fig. 6. Electrical conductivity of latex-based composites, dried at room temperature, as a function of CB concentration (a) and glass transition temperature as a function of percolation threshold (b).

random placement of carbon black once the polymer matrix achieves a liquid-like state, as expected. A plot of log E′ as a function of V_c intercepts 15 vol% CB at a storage modulus of approximately 7 Pa (see Supplementary data), which is essentially a liquid.

Increasing the drying temperature yields dramatic changes in the percolation behavior of all composites, especially BA5. Fig. 7(b) compares electrical conductivity as a function of carbon black concentration for BA5 composites dried at 20 and 80 °C. The percolation threshold increases from 1.5 to 3.6 vol% due to the significant drop in modulus for the BA5 copolymer, from 610 to 0.84 MPa, by increasing the temperature from 20 to 80 °C. The V_c of other composites also increases, but the changes are not as significant. The difference in V_c shrinks as the concentration of butyl acrylate increases because the polymer modulus at room temperature is already close to the rubbery plateau modulus. The percolation threshold increases by 1.52 vol% for BA5.5 and 1.11 vol% for BA6 composites. As expected from the microstructural images (Fig. 5), the electrical conductivity of BA7 shows dissimilar behavior with these other systems. The conductivity of BA7 dried at 80 °C is not measurable until 9.5 vol% CB and the measured values are

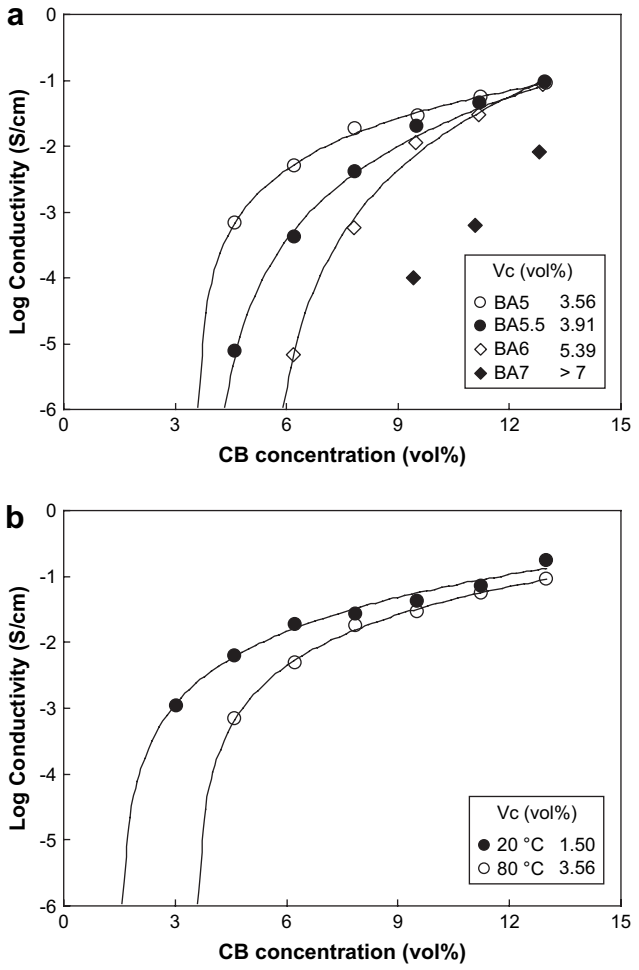

Fig. 7. Electrical conductivity of latex-based composites, dried at 80 °C, as a function of CB concentration (a) and a comparison of BA5 composites dried at 20 and 80 °C (b).

orders of magnitude smaller than those of the other systems. With only three data points, it is not possible to accurately obtain V_c. However, the percolation threshold of BA7 is seemingly higher than 7 vol%. This type of conductivity behavior is more typical of polymer composites with randomly dispersed carbon black [24,29]. BA7 has a T_g that is much lower than the other systems. Low T_g typically means a lower melting point, which makes BA7 act like a viscous liquid at 80 °C and the conductivity trend of BA7 becomes more like that of a melt-based composite.

4. Conclusion

A series of polymer emulsions with different glass transition temperatures were synthesized by varying the ratio of butyl acrylate and methyl methacrylate repeat units. The glass transition temperatures of these latexes were higher than those predicted by the Fox equation due to greater MMA reactivity that likely increased its concentration in the copolymer. Composites made using the emulsion with higher room temperature modulus (due to higher T_g) exhibited a lower percolation threshold and higher electrical conductivity. When the modulus of the polymer is high, the emulsion particles tend to maintain their original shape during the coalescence process. In this case, carbon black particles are more effectively forced into the interstitial space between the polymer particles to form a segregated network at lower concentration. Lower modulus polymer particles easily deform around CB particles and separate them from one another. The V_c of BA5 (the highest modulus polymer) at room temperature is significantly lower than those of the lower modulus composites and the conductivity values are higher. This disparity between BA5 and the other composites is reduced by increasing the drying temperature to 80 °C, where the modulus of BA5 is closer to that of BA5.5 and BA6. The dispersion level of CB in the three composites containing 15 wt% CB is qualitatively the same. When the polymer contains a 7:3 ratio of BA/MMA (BA7), the modulus of the copolymer is 0.1 MPa at 80 °C. CB is more uniformly dispersed in this very soft matrix without formation of a network until much higher concentration. The conductivity behavior of BA7 is similar to that of a randomly dispersed composite produced from solution or melt processing.

Acknowledgments

Authors would like to acknowledge the Texas Engineering Experiment Station (TEES) for financial support of this research.

Appendix. Supplementary data

Supplementary data associated with this article can be found, in the online version, at doi:10.1016/j.polymer.2007.11.035.

References

[1] Hwang J, Muth J, Ghosh T. J Appl Polym Sci 2007;104(4):2410–7.
[2] Wan Y, Wen DJ. Smart Mater Struct 2004;13(5):983–9.
[3] Feller JF, Grohens Y. Synth Met 2005;154(1–3):193–6.
[4] Koscho ME, Grubbs RH, Lewis NS. Anal Chem 2002;74(6):1307–15.
[5] Das NC, Chaki TK, Khastgir D, Chakraborty A. Adv Polym Tech 2001;20(3):226–36.
[6] Klason C, McQueen DH, Kubat J. Macromol Symp 1996;108:247–60.
[7] Voigt B, Rouxel D, McQueen DH, Rychwalski RW. Polym Compos 2005;26(2):144–51.
[8] Souza FG, Sena ME, Soares BG. J Appl Polym Sci 2004;93(4):1631–7.
[9] Dai K, Xu XB, Li ZM. Polymer 2007;48(3):849–59.
[10] Yui H, Wu GZ, Sano H, Sumita M, Kino K. Polymer 2006;47(10):3599–608.
[11] Tchoudakov R, Breuer O, Narkis M, Siegmann A. Polym Eng Sci 1996;36(10):1336–46.
[12] Levon K, Margolina A, Patashinsky AZ. Macromolecules 1993;26(15):4061–3.
[13] Cheah K, Forsyth M, Simon GP. J Polym Sci Part B Polym Phys 2000;38(23):3106–19.
[14] Gubbels F, Blacher S, Vanlathem E, Jerome R, Deltour R, Brouers F, et al. Macromolecules 1995;28(5):1559–66.
[15] Zoldan J, Siegmann A, Narkis M. Polym Eng Sci 2006;46(9):1250–62.
[16] Grunlan JC, Gerberich WW, Francis LF. J Appl Polym Sci 2001;80(4):692–705.
[17] Wang YC, Anderson C. Macromolecules 1999;32(19):6172–9.

[18] Grunlan JC, Mehrabi AR, Bannon MV, Bahr JL. Adv Mater 2004;16(2):150–3.
[19] Hu JW, Li MW, Zhang MQ, Xiao DS, Cheng GS, Rong MZ. Macromol Rapid Commun 2003;24(15):889–93.
[20] Regev O, ElKati PNB, Loos J, Koning CE. Adv Mater 2004;16(3):248–51.
[21] Geblinger N, Thiruvengadathan R, Regev O. Compos Sci Tech 2007;67(5):895–9.
[22] Kim YS, Liao KS, Jan CJ, Bergbreiter DE, Grunlan JC. Chem Mater 2006;18(13):2997–3004.
[23] Kirkpatrick S. Rev Mod Phys 1973;45(4):574–88.
[24] Grunlan JC, Gerberich WW, Francis LF. J Mater Res 1999;14(11):4132–5.
[25] Tang H, Chen XF, Tang AQ, Luo YX. J Appl Polym Sci 1996;59(3):383–7.
[26] Kusy RP. J Appl Phys 1977;48(12):5301–5.
[27] Lee GJ, Suh KD, Im SS. Polym Eng Sci 1998;38(3):471–7.
[28] Feller JF, Linossier I, Levesque G. Polym Adv Technol 2002;13(10–12):714–24.
[29] Tang H, Chen XF, Luo YX. Eur Polym J 1996;32(8):963–6.
[30] Schueler R, Petermann J, Schulte K, Wentzel HP. J Appl Polym Sci 1997;63(13):1741–6.
[31] Octylphenol ethoxylates, <http://www.dow.com/surfactants/products/octyl.htm>; 2007 (accessed 14.11.2007).
[32] Wu J, Winnik MA, Farwaha R, Rademacher J. Macromol Chem Phys 2003;204(16):1933–40.
[33] Liu J, Chew CH, Gan LM, Teo WK, Gan LH. Langmuir 1997;13(19):4988–94.
[34] Chern CS, Hsu H. J Appl Polym Sci 1995;55(4):571–81.
[35] Sperling LH. Introduction to physical polymer science. 4th ed. Hoboken: Wiley and Sons, Inc.; 2006 [chapter 8].
[36] Grunlan JC, Ma Y, Grunlan MA, Gerberich WW, Francis LF. Polymer 2001;42(16):6913–21.
[37] Agarwal N, Farris RJ. Polym Eng Sci 2000;40(2):376–90.